Available online at www.sciencedirect.com
SCIENCE DIRECT®
International Journal of Heat and Mass Transfer 48 (2005) 965–973
International Journal of HEAT and MASS TRANSFER
www.elsevier.com/locate/ijhmt

Structural analysis of turbulent transport in a heated drag-reducing channel flow with surfactant additives

Feng-Chen Li [a,b], Yasuo Kawaguchi [a,*], Koichi Hishida [c]

[a] Turbomachinery Research Group, Energy Technology Research Institute, National Institute of Advanced Industrial Science and Technology, Namiki 1-2-1, Tsukuba 305-8564, Japan
[b] Center for Smart Control of Turbulence, National Maritime Research Institute, Shinkawa 6-38-1, Mitaka, Tokyo 181-0004, Japan
[c] Department of System Design Engineering, Keio University, Yokohama 223-8522, Japan

Received 13 December 2003; received in revised form 2 July 2004
Available online 22 December 2004

Abstract

Turbulence transport features in a heated drag-reducing surfactant solution (CTAC, 30 wppm) channel flow was investigated by simultaneously measuring velocity and temperature fluctuations in the thermal boundary layer. Measurement was made at inlet fluid temperature of 304 K and at three Reynolds numbers (based on channel height, bulk velocity and solvent viscosity): 3.5×10^4, 2.5×10^4 and 1.5×10^4. Structural analysis showed that the drag-reducing additives inhibited the motions associated with ejections of low-momentum fluid away from the wall and sweeps of high-momentum fluid toward the wall (the second and fourth quadrant motion respectively) but had no obvious effect on the outward motion of high-momentum fluid and wall-ward motion of low-momentum fluid (the first and third quadrant motion respectively). The depression of wall-normal turbulent heat flux was due to the decreased contributions of the second and fourth quadrant motions.

Keywords: Channel flow; Surfactant solution; Drag reduction; Heat transfer reduction; Quadrant analysis

1. Introduction

It is known for more than 50 years that small amounts of long-chain polymers or surfactants, when added to turbulent water flows, have a dramatically large macroscopic effect (the so-called Toms effect [1]) on reducing the pressure drop in a pipe flow. Although the drag-reducing polymeric additives and surfactant additives have similar ability to reduce frictional drag, causing drag-reduction (DR) of even more than 80%, polymeric additives are susceptible to an irreversible degradation of the drag-reducing ability in high shear flows (e.g., when driven by a pump) whereas surfactant additives are not. Therefore, surfactant additives are more appropriate for fluid circulating systems, such as hydronic district heating and cooling systems, in which pumping power is necessary. The microstructure in a carefully-made drag-reducing surfactant solution imparts viscoelasticity to the fluid, which is thought to cause DR. Such microstructure is mechanically degraded when it flows through a pump, but it recovers immediately after the high shear is released and this recovery procedure can be repeated any number of times after passing through the pump [2].

* Corresponding author. Tel.: +81 29 861 7257; fax: +81 29 861 7275.
E-mail address: kawaguchi.y@aist.go.jp (Y. Kawaguchi).

0017-9310/$ - see front matter © 2004 Elsevier Ltd. All rights reserved.
doi:10.1016/j.ijheatmasstransfer.2004.09.029

Nomenclature

D	hydraulic diameter of flow channel (m)
H	channel height (m)
Pr	molecular Prandtl number
q	heat flux (K m/s)
Re	Reynolds number based on bulk velocity, channel height and water viscosity
Re_τ	Reynolds number based on friction velocity and half channel height
T	local fluid temperature (K)
T_b	bulk temperature (K)
T_{in}	inlet fluid temperature (K)
T_w	heated wall temperature (K)
T_τ	friction temperature (K)
U	the streamwise velocity (m/s)
u	the streamwise velocity fluctuation (m/s)
u_τ	friction velocity (m/s)
v	the wall-normal velocity fluctuation (m/s)
x	coordinate in the streamwise direction (m)
y	coordinate in the wall-normal direction (m)

Greek symbols

Θ	local mean temperature difference, $\equiv T_w - T$ (K)
θ	temperature difference fluctuation (K)
τ	shear stress (Pa)

Superscripts

$(\cdot)'$	root-mean-square value
$(\cdot)^+$	normalized with wall units

In a heated drag-reducing flow produced by additives, heat transfer reduction (HTR) of the same order of DR also occurs. The reduction of heat transfer in heat exchangers is an important issue in a hydronic heat transportation system. Hence, it is important to clarify the mechanism of HTR as well as DR in solving the conflicting problems between HTR and DR (DR is beneficial to save pumping energy whereas HTR reduces the efficiency of heat exchangers), so as to broaden the applications of drag-reducing additives.

In experimental studies of a cationic surfactant solution (aqueous solution of cetyltrimethyl ammonium chloride, CTAC) channel flow [3–5], the characteristics of DR and HTR, turbulence structures and turbulence transport for momentum have been investigated. From the previous experimental results, including those obtained with drag-reducing surfactant and polymeric flows by other researchers [6–10], a consensus understanding of the DR phenomena has been achieved, such as the extension of inner layer and upward shift of the mean velocity in the log-law layer of the velocity profile, increase in the streamwise velocity fluctuation intensity (normalized with the friction velocity) near the wall, decrease in the wall-normal velocity fluctuation intensity, depression in the Reynolds shear stress, decrease in turbulent kinetic energy production, decrease in frequency of occurrence of bursting events, enlargement of distance between the near-wall low-speed streaks, and variations on the power spectrum of the streamwise velocity fluctuations, i.e., the decrease at high frequencies and increase at low frequencies, compared with a Newtonian fluid flow.

Recently, the characteristics of thermal turbulence structures and turbulence transport for heat in a heated CTAC solution channel flow were also investigated [11–13]. The results will be summarized in Section 3. In this paper, we continue experimental investigation of the behaviors of HTR as well as DR in a heated drag-reducing surfactant solution flow, focusing on the structural analysis of the wall-normal turbulence transports for momentum and heat influenced by the drag-reducing surfactant additives.

2. Overview of the experiment

A closed-circuit water channel is used in the present study. The 10 m-long channel is made of transparent acrylic resin (except for the heating section), with a height (H) of 0.04 m and a width of 0.5 m. The heating section (consisting of backplate, heater and copper plate) is 0.9 m long, located at 8.2 m (measured from the front edge) downstream from the channel entrance, as shown in Fig. 1. The measurement station is in a central plane in the spanwise direction and is located at 0.8 m (20H) downstream from the front edge of the heating section, and thus 9.0 m (225H) downstream from the channel

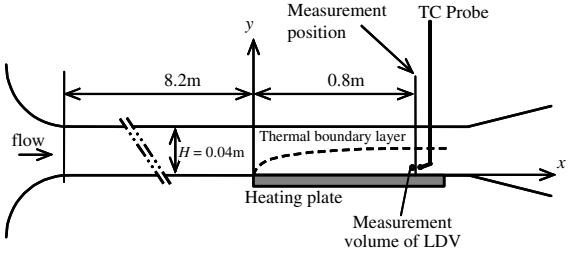

Fig. 1. Schematic diagram of the test section.

entrance. A constant wall-heated flux is supplied on the heating copper plate.

It has been documented that the length needed for fully developed flow of drag-reducing surfactant solutions is longer than that for water flow. Gasljevic and Matthys [14] addressed that the point at $190D$ (D is the hydraulic diameter) downstream in their experiments was close to being hydrodynamically fully developed in a drag-reducing surfactant solution flow. In the present study, the measurement station is located $225H$ downstream, corresponding to about $122D$. Hence, it is expected that the flow is hydrodynamically fully developed at this position. To be thermally fully developed, drag-reducing flow by additives needs much longer distance [14]. However, in many heat transfer measurements, it shows that the Nusselt number only has large gradient with respect to the streamwise distance in a short entrance length for a drag-reducing flow by additives. For example, in the experimental study of [3], the Nusselt number changed significantly only up to about $10H$ for a 30 ppm CTAC solution flow. After $10H$, the local Nusselt number slightly changed with downstream distance (see Fig. 6 in [3]). It is then believed that at location of $20H$ downstream from the entrance of heating section for the present case, the variation of thermal field has no much effect on the measurement although the flow is still thermally developing.

A dilute aqueous solution of CTAC/NaSal is used as the drag-reducing fluid. The concentration of CTAC is 30 wppm. NaSal (sodium salicylate), with the same concentration as that of CTAC, provides counter ions. Tap water is used as the solvent. The thermo-physical properties of solvent are used for data reduction. A water flow is also tested for a comparison.

The streamwise and wall-normal velocity components, u and v respectively, are measured with a laser Doppler velocimetry (LDV), and the temperature fluctuation at the same location in the fluid is measured with a fine-wire ($\varnothing 2.54\times10^{-5}$ m) K-type thermocouple (TC) probe. The time constant of the TC probe is estimated to be about 5.0×10^{-4} s at the tested conditions (at the same conditions, the Kolmogorov time scale and Obukhov–Corrsin time scale are 2.7×10^{-3} s and 7.6×10^{-4} s respectively). The separation distance between the junction of the TC wires and the measurement volume of LDV is kept at 2.0×10^{-4} m (about 4 times the Kolmogorov length scale, and 5.5 and 3.0 wall units for water and CTAC solution flows respectively). The Doppler signals are processed with two synchronized burst-spectrum-analyzers (BSAs). Signals from the TC probe are sampled with an analog-to-digital converter (AD-converter) after being amplified and filtered. The AD-converter is triggered by the master BSA. The signals of velocity and temperature fluctuations are simultaneously recorded and transferred to a personal computer.

The back surface temperatures of the copper plate are measured with K-type TCs. The surface temperature attaching to the fluid is estimated based on the measurement. All the TCs including the fine-wire TC probe are calibrated and found to have uncertainty of ±0.1 K. The estimated relative uncertainties of measured values for velocity and temperature are ±0.2% and ±0.3% respectively.

The experimental procedure and data processing method are the same as those previously conducted. Table 1 lists the test conditions. Note that y^+_{CL} (normalized with the inner wall variables) in Table 1 corresponds to $y/(H/2) = 1$. The solvent viscosity is used for data-processing throughout this paper, since the measured viscosity of solution as dilute as 30 ppm was almost the same as that of water [13].

Detailed descriptions of the experiment can be found elsewhere [12].

3. Results and discussion

In the previous paper [13], we reported the characteristics of thermal as well as hydrodynamic turbulence statistics and turbulence transport for heat as well as momentum in a heated 30 ppm CTAC solution flow. At high DR or HTR level, a large temperature gradient appeared at about $10 < y^+ < 50$, which can also be thought of as a modification of the temperature profile similar to that of the inner layer of the streamwise velocity profile. The peaks of both profiles of temperature fluctuation intensity and the streamwise turbulent heat flux were enhanced, whereas the turbulent heat flux in the wall-normal direction, $-\overline{v^+\theta^+}$, was depressed throughout the measured range in the drag-reducing CTAC solution flow. Furthermore, the depression of

Table 1
Test parameters

Cases	T_{in} (K)	Re	u_τ (m/s)	T_τ (K)	DR (%)	HTR (%)	y^+_{CL}
Water	304	2.5×10^4	0.025	0.020	–	–	262.9
CTAC (CA)	304	3.5×10^4	0.027	0.018	33.0	20.2	249.8
CTAC (CB)	304	2.5×10^4	0.012	0.041	70.0	77.3	121.1
CTAC (CC)	304	1.5×10^4	0.009	0.034	65.1	77.0	86.9

$-\overline{v^+\theta^+}$ occurred in a similar way with that of the Reynolds shear stress, $-\overline{u^+v^+}$, i.e., the occurrence of decorrelation between v and θ compared with the occurrence of decorrelation between u and v, in addition to the decrease of the fluctuation intensity v'. The turbulence production of turbulent kinetic energy and that of temperature variance are reduced in the drag-reducing CTAC solution flow. The estimated power spectrum of temperature fluctuations implies that the drag-reducing surfactant additive depresses the turbulence at high frequencies or at small scales, whereas it increases the turbulent energy at low frequencies or at large scales. The eddy diffusivities for momentum and heat in the CTAC solution flows are both decreased. The turbulent Prandtl number profiles deviated from that of the water flow in the region corresponding to the high-temperature-gradient layer. The value of the turbulent Prandtl number in this layer becomes close to the molecular Prandtl number of the solvent, which is due to the laminarization of the flow by the drag-reducing additives.

In order to clarify the behaviors of turbulence transports, and so the mechanisms of DR and HTR, structural analyses have been performed for the turbulence transport terms for both momentum and heat. The following sections describe the shear stress balance, wall-normal turbulent heat flux balance, quadrant analyses of $-\overline{uv}$ and $-\overline{v\theta}$. Note that the measurement technique employed in the present experiment shows good reproducibility of the quantities illustrated below. For example, for water flows at $Re = 2.36 \times 10^4$ and $Re = 2.5 \times 10^4$ reported in [12] and [13] respectively, the differences between the two independently measurement by using the same technique were less than about 0.5% for U^+ (indicating a good reproducibility of $\partial U^+/\partial y^+$), 8% for Θ^+ (indicating a good reproducibility of $\partial \Theta^+/\partial y^+$), 11% for $-\overline{u^+v^+}$ and 25% for $-\overline{v^+\theta^+}$, and the difference was

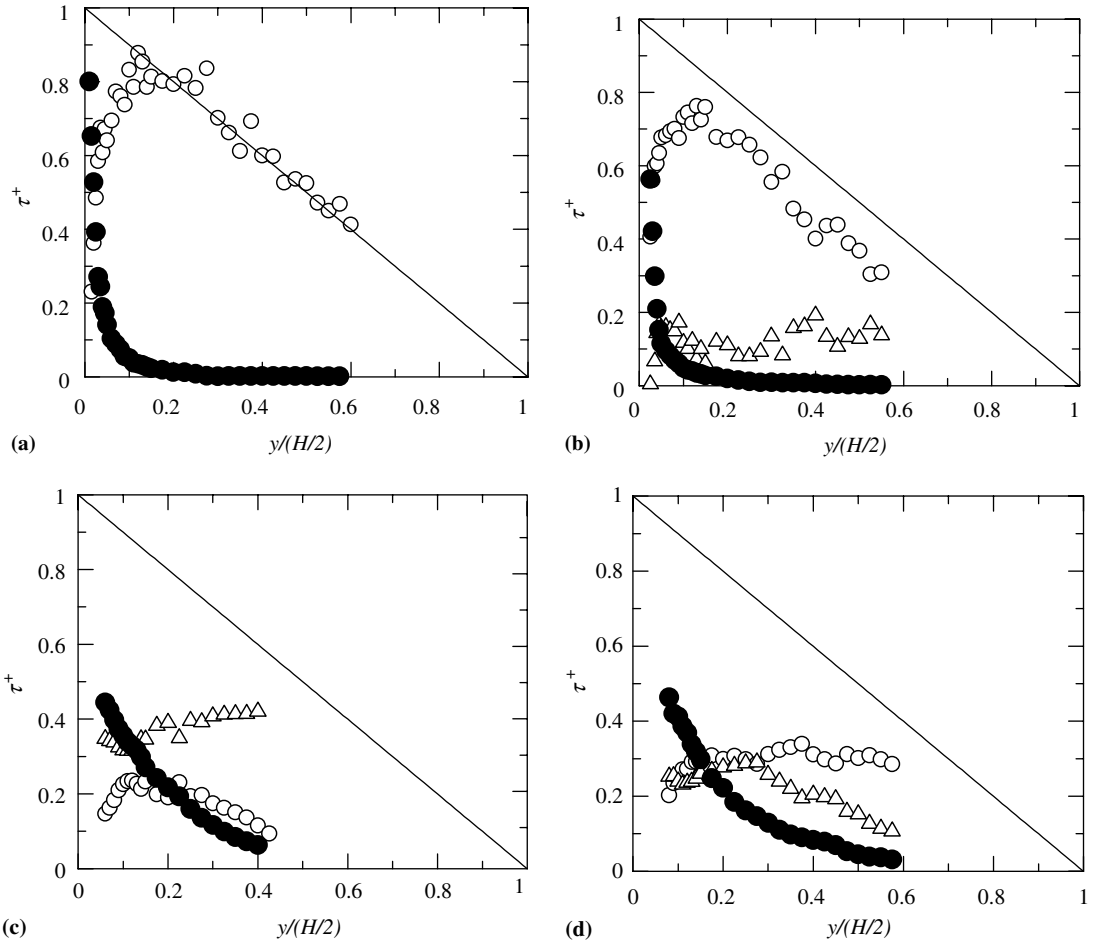

Fig. 2. Shear stress contributions as a function of $y/(H/2)$: the solid line represents the total shear stress, τ_m^+; ○, the Reynolds shear stress, τ_T^+; ●, viscous shear stress, τ_V^+; △, elastic shear stress, τ_E^+. (a) water; (b) CA; (c) CB and (d) CC.

thought to be mainly due to the different sampling spaces between the two measurements.

3.1. Shear stress balance

In the investigation of drag-reducing flow by polymeric or surfactant additives, the so-called Reynolds shear stress deficit has been repeatedly observed. An elastic stress or Reynolds shear stress deficit term is therefore introduced into the total shear stress balance [8,10], i.e.,

$$\tau_m = \tau_T + \tau_V + \tau_E \quad (1)$$

where τ_m represents the total shear stress, τ_T the Reynolds shear stress, τ_V viscous shear stress and τ_E elastic stress. For a hydrodynamically fully developed two dimensional channel flow, normalized with inner wall variables, the total shear stress balance becomes,

$$\tau_m^+ = 1 - y^+/Re_\tau = \tau_T^+ + \tau_V^+ + \tau_E^+ \quad (2)$$

$\tau_T^+ = -\overline{u^+v^+}$ is obtained from the instantaneous streamwise and wall-normal velocity components measured by LDV. The estimated uncertainties of $-\overline{uv}$ at a 95% confidence level is <0.7%. $\tau_V^+ = \partial U^+/\partial y^+$ is calculated from

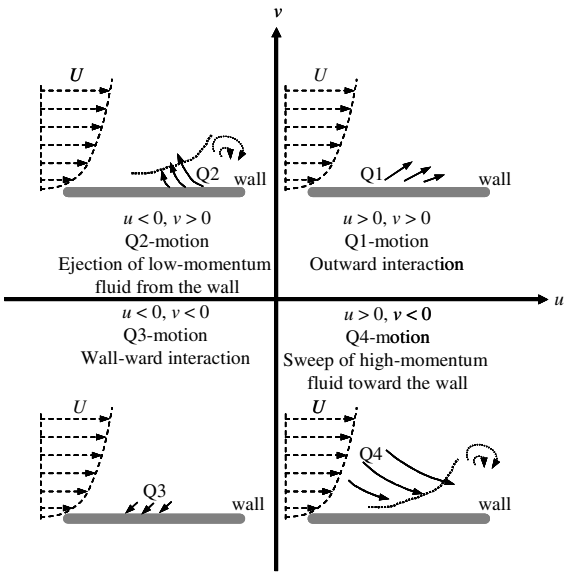

Fig. 3. Schematic diagram of the categorization of turbulent fluid motions (quadrant motions). The viewer is moving with the fluid in the u–v coordinate system. Thus, motions in the streamwise direction represent high-momentum fluid, and opposite the streamwise direction represent low-momentum fluid.

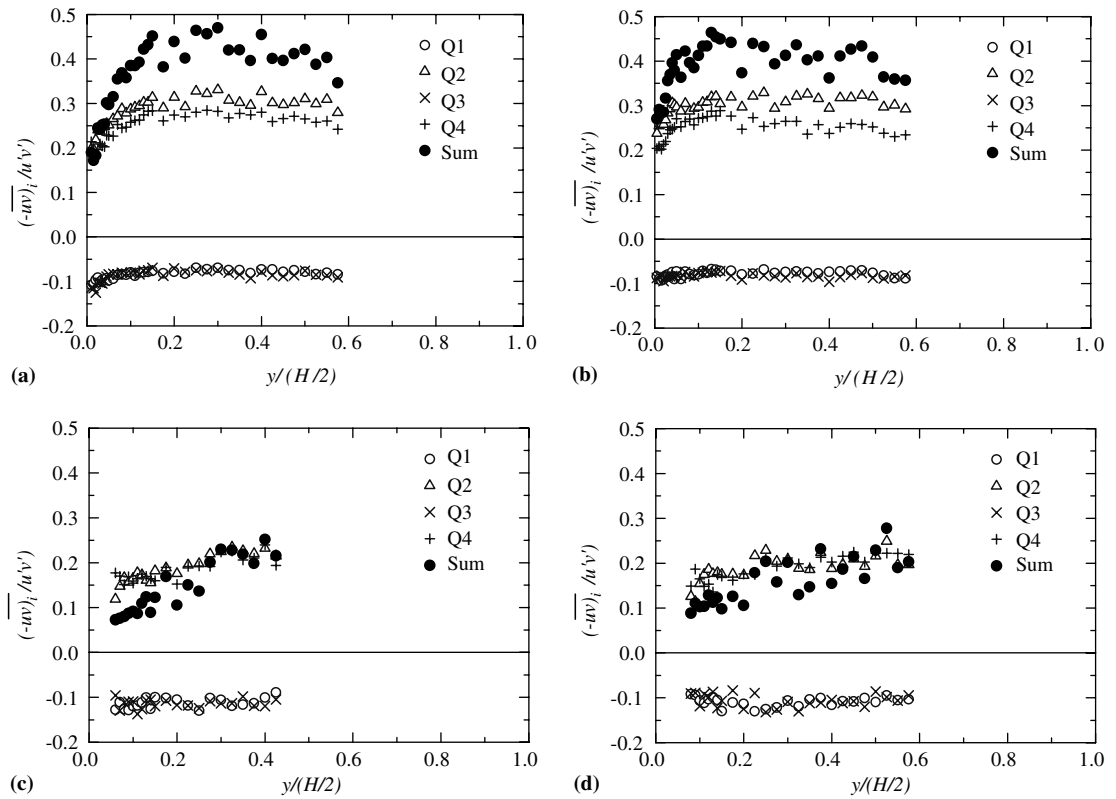

Fig. 4. Fractional contributions of the Reynolds shear stress from different quadrant motions: (a) water; (b) CA; (c) CB and (d) CC.

the measured time–mean velocity profile. The mean velocity profile, U^+ versus y^+, is at first regressed by means of least-square method, and then τ_V^+ is calculated from the smoothed profile of U^+. Based on root-sum-square method [15], the estimated uncertainty of τ_V^+ is ±10.1%. τ_E^+ is determined by subtracting the measured τ_T^+ and the calculated τ_V^+ from the total shear stress, τ_m^+, and has an uncertainty of ±10.7%.

In Fig. 2, the measured and calculated shear stresses for both water and CTAC solution flows are plotted. In water flow, the elastic stress is zero and the sum of τ_T^+ and τ_V^+ is equal to the total shear stress. In the drag-reducing flows, as shown in Fig. 2b–d, the sum of τ_T^+ and τ_V^+ no longer equates to τ_m^+; the contribution of elastic stress, τ_E^+, to τ_m^+ occurs, which is named as the occurrence of "Reynolds stress deficit". The elastic stress τ_E^+ increases with an increase in DR level.

3.2. Quadrant analysis of Reynolds shear stress

Quadrant analysis [16] of $-\overline{uv}$ is conducted in order to provide the detailed information of the contribution to the total turbulence production from various events occurring in the turbulent flows, and to provide information on the influence of drag-reducing surfactant additives on such contributions. Fig. 3 schematically shows the categorization of fluid motions according to the signs of u and v. The contribution of each quadrant to $-\overline{uv}$ is calculated with u and v only located in the individual quadrant in the velocity fluctuation coordinates (u, v), designated as $-\overline{uv}_i$ for the ith quadrant, where $i = 1, 2, 3$ and 4. In the first quadrant, $u > 0$ and $v > 0$, representing outward interactions of fluid (outward motion of high-momentum fluid, Q1 motion); the second quadrant, $u < 0$ and $v > 0$, contains ejections of low-

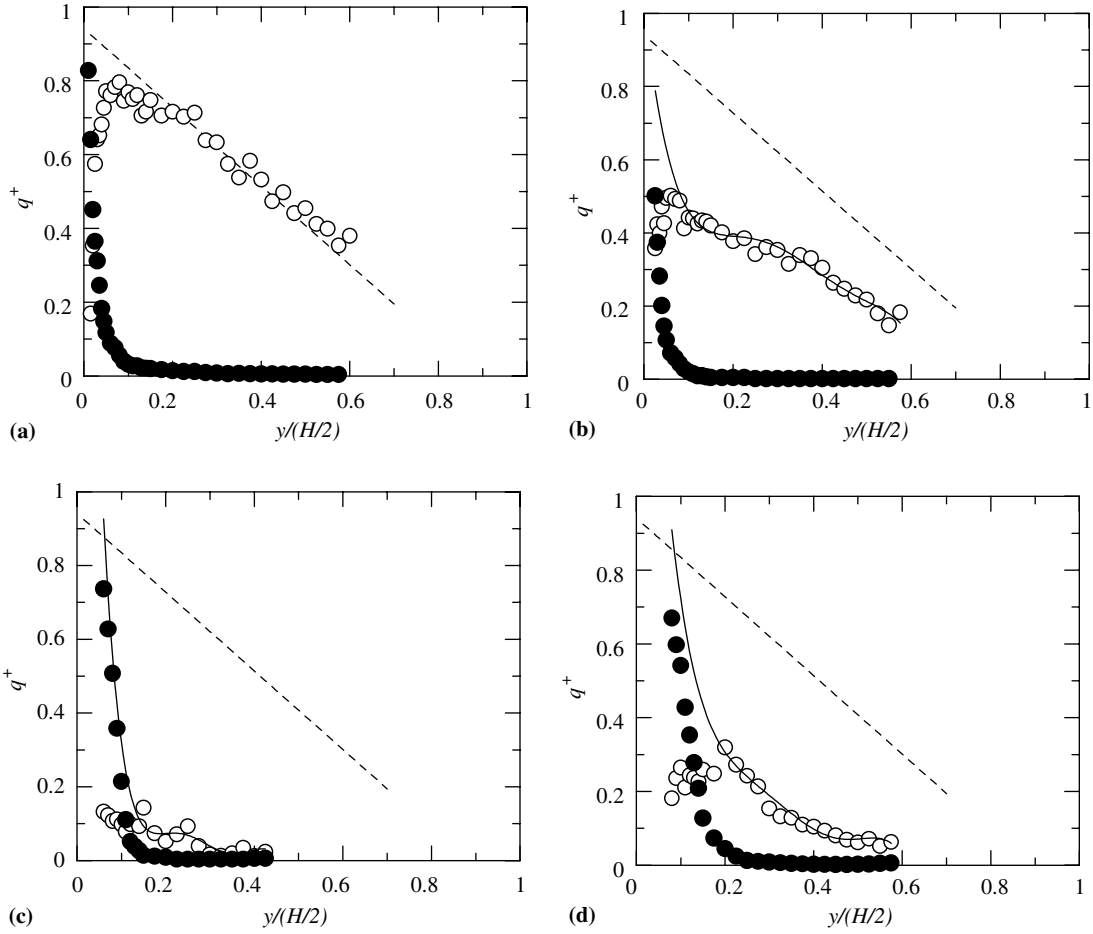

Fig. 5. Turbulent heat flux contributions in the wall-normal direction as a function of $y/(H/2)$: the dash line represents the measured total heat flux normal to the wall for water flow (thermally developing flow), $(q_m^+)_W$; the solid line represents the measured total heat flux in the wall-normal direction in CTAC solution flows, $(q_m^+)_C$; ○, the wall-normal turbulent heat flux, q_T^+; ●, the conductive heat flux, q_C^+. (a) Water; (b) CA; (c) CB and (d) CC.

moment fluid from the wall (Q2 motion); the third quadrant, $u < 0$ and $v < 0$, contains wall-ward interactions of fluid (wall-ward motion of low-momentum fluid, Q3 motion) and the fourth quadrant, $u > 0$ and $v < 0$, contains sweeps of high-moment fluid toward the wall (Q4 motion).

Fig. 4 plots the distributions of $-\overline{uv}_i$ ($i = 1, 2, 3$ and 4) and the sum, $-\overline{uv} = \sum_{i=1}^{4} -\overline{uv}_i$. In water flow, Q2 and Q4 motions are dominant in generating the turbulent shear stress, as shown in Fig. 4a. For all the three cases of CTAC solution flow, however, the contributions of Q2 and Q4 motions vary significantly. With the increase of DR level, both $-\overline{uv}_2$ and $-\overline{uv}_4$ are increasingly depressed, whereas $-\overline{uv}_1$ and $-\overline{uv}_3$ have almost no differences from those in water flow, as shown by comparing Fig. 4b–d with Fig. 4a. Thus, the sum, $-\overline{uv}$, i.e., the Reynolds shear stress, decreases in the drag-reducing flow. This indicates that the drag-reducing surfactant additives inhibit the processes of ejection of low-momentum fluid from the wall and the sweep of high-momentum fluid toward the wall, but do not affect the processes of both outward and wall-ward interactions of fluid.

3.3. Balance of wall-normal heat flux from heated wall to liquid

The heat flux contributions in the wall-normal direction for both water and CTAC solution flows are shown in Fig. 5. The dash line in Fig. 5a–d represents the measured total heat flux normal to the wall for water flow, $(q_m^+)_W = q_T^+ + q_C^+$, in the present study, where q_T^+ is the wall-normal turbulent heat flux, q_C^+ the conductive heat flux. $q_T^+ = -\overline{v^+\theta^+}$ is obtained directly from the simultaneously measured v and θ. The measured total heat flux in CTAC solution flows, $(q_m^+)_C = q_T^+ + q_C^+$, is plotted by the solid line (smoothed) in Fig. 5b–d. The estimated uncertainty of q_T^+ at a 95% confidence level is <5.5%. $q_C^+ = (1/Pr) \cdot (\partial\Theta^+/\partial y^+)$ is calculated from the measured time–mean temperature profile (the procedure is similar to that performed for τ_V^+). The estimated uncertainty of q_C^+ is ±8.6%.

In [3], it was obtained that the profiles of the measured Nusselt number versus the downstream distance for a 30 ppm CTAC solution flow and water flow were similar in shape, i.e., they were nearly parallel to each other everywhere, and the Nusselt numbers at a

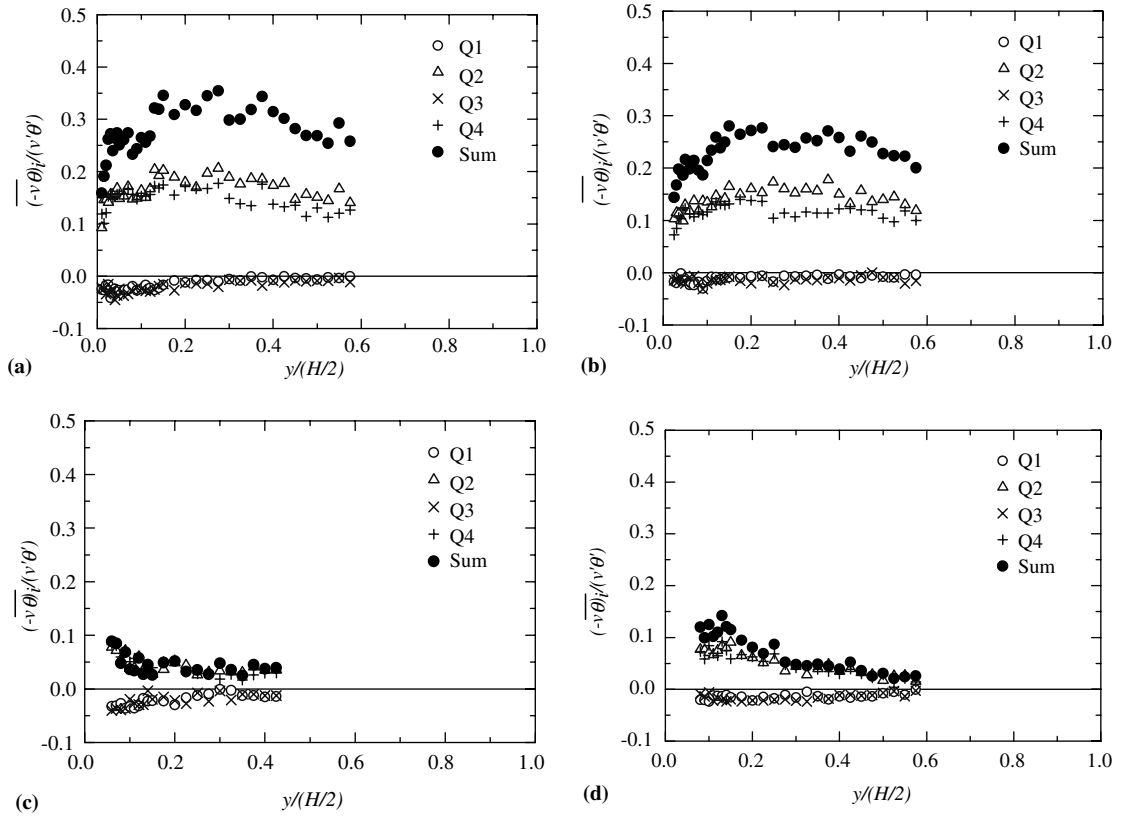

Fig. 6. Fractional contributions of wall-normal turbulent heat flux from different quadrant motions: (a) water; (b) CA; (c) CB and (d) CC.

streamwise location of $20H$ only slightly changed with downstream distance. On the other hand, we also obtained that the turbulent Prandtl numbers in the thermal boundary layer were almost the same in both 30 ppm CTAC solution flow and water flow [13]. These indicate that the developing situation of thermal field for both water flow and drag-reducing CTAC solution flow could be similar with each other at location of $20H$ downstream from the entrance of heating section. By comparing with the measured profile of $(q_m^+)_W$ in water flow, the typical characteristics of turbulence transport for heat in a drag-reducing CTAC solution flow in the thermally developing region can thus be investigated.

As compared with water flow, the drag-reducing CTAC solution flow shows quite different characteristics of heat fluxes normal to the wall in the developing thermal boundary layer (Fig. 5b–d), although the measurements are performed at the same streamwise location. The profile of q_T^+ in a drag-reducing flow is increasingly depressed with the HTR level throughout the measured range, which has been reported by Li et al. [12,13]. The profile of q_C^+ with similar value moves away from the wall compared with water flow. Note that, q_C^+ will decrease with further decreasing the distance from the heated wall surface. Kawaguchi et al. [11] and Li et al. [12] plotted the mean temperature in a broader range (closer to the heated wall) and observed that the temperature gradient was quite low near the wall, indicating the existence of a local high-heat-diffusivity layer. The profile of $(q_m^+)_C$ is increasingly deviated (depressed) from that of $(q_m^+)_W$ with HTR level. The decrease in q_T^+, consequently the decrease in $(q_m^+)_C$ directly results in the decrease in heat transfer rate. In a drag-reducing solution flow, the additives inhibit eddy motions normal to the wall in a turbulent channel flow, and so turbulence transport for heat as well as for momentum is inhibited because the turbulent eddy motions also play essential roles in thermal turbulence transport.

3.4. Quadrant analysis of wall-normal turbulent heat flux

Quadrant analysis is also conducted for the wall-normal turbulent heat flux, $-\overline{v\theta}$, to understand the behavior of turbulence transport for heat in a drag-reducing flow. By calculating the fractional contributions, $-\overline{v\theta}_i$ ($i = 1, 2, 3$ and 4) to $-\overline{v\theta}$ from different quadrant motions categorized in the (u, v) plane, the influences of drag-reducing surfactant additives on thermal turbulence transport during different events, i.e., ejection, sweep and interactions, are investigated.

Fig. 6 shows the results of quadrant analyses of $-\overline{v\theta}$ for both water and CTAC solution flows. In water flow, the contributions of Q2 and Q4 motions (ejection and sweep) to $-\overline{v\theta}$ are also predominant (Fig. 6a). The negative contributions of Q1 and Q3 motions (outward and wall-ward interactions) are quite low in absolute value. In the heated CTAC solution flows, it can be seen that the fractional contributions of Q2 and Q4 motions are greatly decreased at high HTR level, whereas those of Q1 and Q3 motions change little compared with water flow, which results in the depression of the wall-normal turbulent heat flux, i.e., the sum, $-\overline{v\theta} = \sum_{i=1}^{4} -\overline{v\theta}_i$.

4. Conclusions

The following main conclusions are drawn from the present study:

(1) An elastic stress occurs in a drag-reducing solution flow, which increases with DR level.
(2) The drag-reducing additives inhibit the processes of ejection of low-speed fluid from the wall and the sweep of high-speed fluid towards the wall, but do not affect the processes of both outward and wall-ward interactions of fluid, causing the decrease of $-\overline{uv}$.
(3) $-\overline{v\theta}$ is also strongly decreased in a heated CTAC solution flow, which results in a decrease of total heat flux normal to the wall, causing HTR.
(4) Quadrant analysis shows that the depression of $-\overline{v\theta}$ results from the decreased contributions of the second and fourth quadrant motions, which is similar to the behavior for $-\overline{uv}$.

Acknowledgments

This research was carried out as a research project of the Center for Smart Control of Turbulence with the financial support of the Ministry of Education, Culture, Sports, Science and Technology (MECSST).

References

[1] B.A. Toms, Some observation on the flow of linear polymer solutions through straight tubes at large Reynolds number, in: Proceedings of the first International Congress of Rheology, North Holland, Amsterdam, vol. 2, 1949, pp. 135–141.
[2] J.L. Zakin, J. Myska, Z. Chara, New limiting drag reduction and velocity profile asymptotes for nonpolymeric additives systems, AIChE J. 42 (1996) 3544–3546.
[3] P.-W. Li, Y. Kawaguchi, H. Daisaka, A. Yabe, K. Hishida, M. Maeda, Heat transfer enhancement to the drag-reducing flow of surfactant solution in two-dimensional channel with mesh-screen inserts at the inlet, Trans. Amer. Soc. Mech. Eng., J. Heat Transfer 123 (2001) 779–789.
[4] P.-W. Li, Y. Kawaguchi, A. Yabe, Transitional heat transfer and turbulent characteristics of drag-reducing flow

through a contracted channel, J. Enhanced Heat Transfer 8 (2001) 23–40.

[5] Y. Kawaguchi, T. Segawa, Z. Feng, P.-W. Li, Experimental study on drag-reducing channel flow with surfactant additives—spatial structure of turbulence investigated by PIV system, Int. J. Heat Fluid Flow 23 (2002) 700–709.

[6] M.D. Warholic, G.M. Schmidt, T.J. Hanratty, The influence of a drag-reducing surfactant on a turbulent velocity field, J. Fluid Mech. 388 (1999) 1–20.

[7] T. Wei, W.W. Willmarth, Modifying turbulent structure with drag-reducing polymer additives in turbulent channel flows, J. Fluid Mech. 245 (1992) 619–641.

[8] J.M.J. Den Toonder, M.A. Hulsen, G.D.C. Kuiken, F.T.M. Nieuwstadt, Drag reduction by polymer additives in a turbulent pipe flow: numerical and laboratory experiments, J. Fluid Mech. 337 (1997) 193–231.

[9] G. Hetsroni, J.L. Zakin, A. Mosyak, Low-speed streaks in drag-reduced turbulent flow, Phys. Fluids 9 (1997) 2397–2404.

[10] P.K. Ptasinski, B.J. Boersma, F.T.M. Nieuwstadt, M.A. Hulsen, B.H.A.A. Van den Brule, J.C.R. Hunt, Turbulent channel flow near maximum drag reduction: simulations, experiments and mechanisms, J. Fluid Mech. 490 (2003) 251–291.

[11] Y. Kawaguchi, H. Daisaka, A. Yabe, K. Hishida, M. Maeda, Structure of thermal boundary layer and heat transfer characteristics in drag reducing flow with surfactant additive, Trans. Jpn. Soc. Mech. Eng. 67 (B) (2001) 1311–1318.

[12] F.-C. Li, Y. Kawaguchi, K. Hishida, Simultaneous measurements of velocity and temperature fluctuations in thermal boundary layer in a drag-reducing surfactant solution flow, Exp. Fluids 36 (2004) 131–140.

[13] F.-C. Li, Y. Kawaguchi, K. Hishida, Investigation on the characteristics of turbulent transport for momentum and heat in a drag-reducing surfactant solution flow, Phys. Fluids 16 (2004) 3281–3295.

[14] K. Gasljevic, E.F. Matthys, Experimental investigation of thermal and hydrodynamic development regions for drag-reducing surfactant solution, Trans. Amer. Soc. Mech. Eng. J. Heat Transfer 119 (1997) 80–88.

[15] S.J. Kline, F.A. McClintok, Describing uncertainties in single-sample experiments, Mech. Eng. (Amer. Soc. Mech. Eng.) 75 (1953) 3–8.

[16] S.S. Lu, W.W. Willmarth, Measurements of the structure of the Reynolds stress in a turbulent boundary layer, J. Fluid Mech. 60 (1973) 481–511.